Liu *et al. Bioresour. Bioprocess. (2018) 5:23*
https://doi.org/10.1186/s40643-018-0209-5

Bioresources and Bioprocessing

RESEARCH

Open Access

2-Hydroxy-4-(3′-oxo-3′*H*-benzofuran-2′-yliden)but-2-enoic acid biosynthesis from dibenzofuran using lateral dioxygenation in a *Pseudomonas putida* strain B6-2 (DSM 28064)

Xin Liu†, Weiwei Wang†, Haiyang Hu, Xinyu Lu, Lige Zhang, Ping Xu and Hongzhi Tang*

Abstract

Background: Benzofuran and its derivatives contain central pharmacophores and are important structures in medicinal chemistry. Chemical synthesis of benzofuran rings often requires expensive catalysts and stringent operational conditions. Biosynthesis is recognized as a promising way to save energy and produce valuable compounds. Dioxin biodegradation pathways can form several benzofuran derivatives, and these pathways may be a better choice for further synthesis of important biological compounds. 2-Hydroxy-4-(3′-oxo-3′*H*-benzofuran-2′-yliden)but-2-enoic acid (HOBB), a benzofuran derivative, can be biosynthesized from dibenzofuran (DBF) through co-metabolic degradation in a lateral dioxygenation pathway.

Results: Efficient biosynthesis of HOBB was observed using whole cells of *Pseudomonas putida* strain B6-2. After cultivation in LB medium containing biphenyl, the cells were suspended to an OD_{600} of 5 to conduct biosynthesis in the presence of 0.5-mM DBF at pH 7 for 8 h. The bacterial cells were used twice to degrade approximately 0.70-mM DBF, and in batch process, accumulated about 0.29-mM HOBB. HOBB could be easily purified from the reaction with ethyl acetate using the neutral-acid extraction method, and 13.58 ± 0.31 mg of HOBB was obtained from 22.49 ± 0.74-mg DBF with an overall production yield of 60.4% (w/w). The product HOBB, which is a yellow powder, could be detected and identified by LC–MS, GC–MS, and NMR.

Conclusions: In this study, a new biological route was developed to produce HOBB from DBF using whole cells of *P. putida* B6-2 (DSM 28064). The biosynthesis of HOBB may contribute to studies of the DBF lateral pathway and provide a new green route for synthesizing benzofuran derivatives with pharmacological activities.

Keywords: Biosynthesize, *Pseudomonas putida*, Lateral dioxygenation, HOBB

Background

Many natural products with biological activities are benzofuran heterocycles (Nevagi et al. 2015; Yeung 2012). Benzofuran and its derivatives are central pharmacophores and important structures in medicinal chemistry (Fig. 1a) because of their broad spectra of pharmacological activities (Khanam and Shamsuzzaman 2015). These products contain mono and fused benzofuran rings in conjunction with other heterocycle compounds (Nevagi et al. 2015). For example, 4-hydroxy-3-methyl-6-phenylbenzofuran-2-carboxylic acid ethyl ester was reported as an anti-tumor agent (Hayakawa et al. 2004a, b), a series of imidazopyridinylbenzofurans have been identified as potent, non-peptide antagonists of angiotensin II (Judd et al. 1994), and other benzofuran derivatives

*Correspondence: tanghongzhi@sjtu.edu.cn
†Xin Liu and Weiwei Wang have contributed equally to this work
State Key Laboratory of Microbial Metabolism, and School of Life Sciences & Biotechnology, Shanghai Jiao Tong University, Shanghai 200240, People's Republic of China

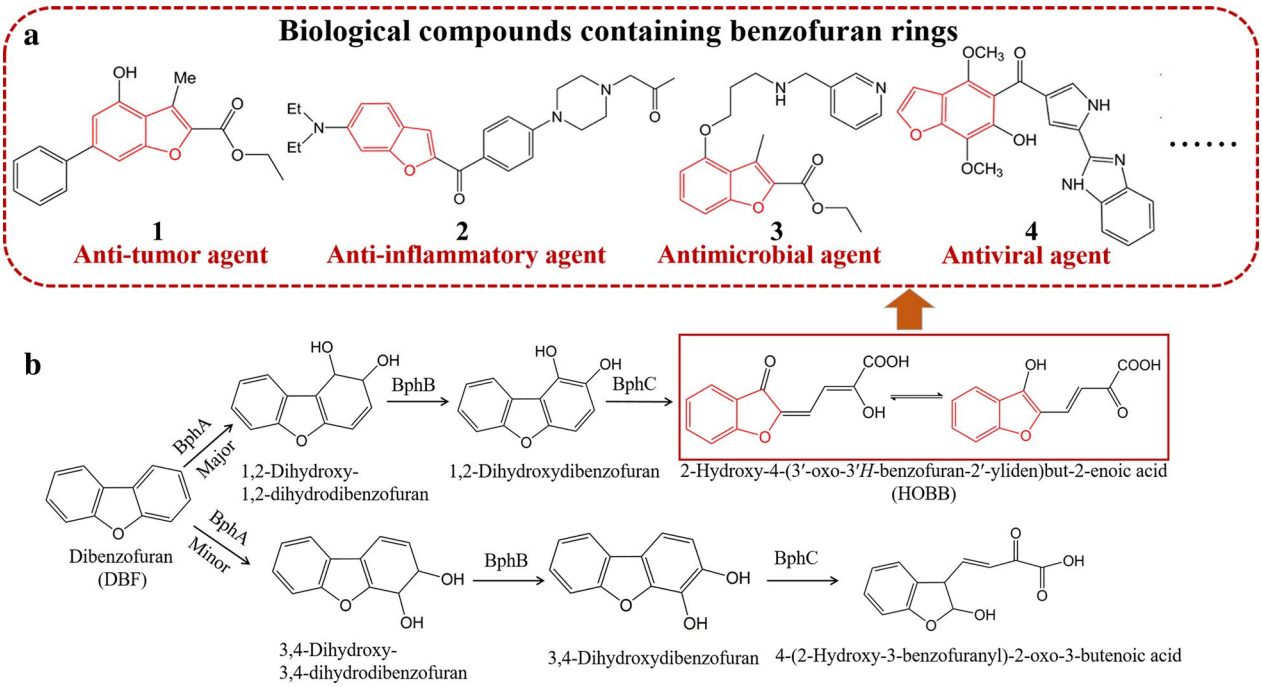

Fig. 1 Benzofuran derivatives that are pharmacological agents and products of the DBF biodegradation pathway. **a** Compounds with biological activities used in pharmacology. (**1**) 4-Hydroxy-3-methyl-6-phenylbenzofuran-2-carboxylic acid ethyl ester showed selective and potent cytotoxicity against tumors (Hayakawa et al. 2004a, b). (**2**) Compound **2** was found to be the most potent anti-inflammatory agent (Ma et al. 2016). (**3**) RO-09-4609 is a basic antifungal agent (Nevagi et al. 2015). (**4**) Hit compound **4** has a high therapeutic index in HIV inhibition (Khanam and Shamsuzzaman 2015). **b** HOBB (a benzofuran derivative) is the main product of DBF catalysis by BphA, BphB, and BphC in the lateral degradation pathway of *Pseudomonas putida* strain B6-2

are used as antimicrobial, antiviral, anti-inflammation, and anti-hyperlipidemic agents (Aswathanarayanappa et al. 2013; Khanam and Shamsuzzaman 2015; Ma et al. 2016; Nevagi et al. 2015). In many studies, benzofuran derivatives are first synthesized from a benzofuran ring (Aswathanarayanappa et al. 2013; Salih et al. 2007), and then, biological agents are further chemically synthesized from the benzofuran derivatives (El-Zahar et al. 2011; Galal et al. 2009; Ma et al. 2016). Chemical synthesis of benzofuran rings is expensive, because transition metals are used, and the operational conditions are stricter than those used for biosynthesis (Cacchi et al. 2002; Oppenheimer et al. 2007; Trost and Mcclory 2007). Using biocatalysts for the industrial synthesis has been recognized as an environmental-friendly synthetic method (Ishige et al. 2005).

Dioxins, which are typically formed as undesired by-products of industrial and municipal activities (Jaiswal et al. 2011), are toxic, carcinogenic, mutagenic, and persistent environmental pollutants (Hiraishi 2003; Ritchie 2000). Their removal from the environment is very challenging. Many physicochemical techniques such as thermal remediation and photo-degradation have been used to remove dioxins; however, these methods are not suitable for treating large areas of dioxin-contaminated soil and sediments (Hiraishi 2003). Bioremediation techniques using specific microorganisms or microbial consortia are more effective and relatively inexpensive, and have gained increasing attention since the 1970s (Matsumura and Benezet 1973; Ward and Matsumura 1978; Wilkes et al. 1996; Wittich 1998). Dibenzofuran (DBF) has been studied as a model dioxin-like compound, and the initial steps of its biodegradation can be categorized into two main pathways: angular dioxygenation and lateral dioxygenation. Numerous bacteria that use DBF as their sole carbon source via angular dioxygenation have been isolated (Hong et al. 2004; Nojiri et al. 2002; Wittich et al. 1992). Other microorganisms can conduct co-metabolic degradation of DBF via lateral dioxygenation when cultivated with biphenyl (BP) or naphthalene (Becher et al. 2000; Kaiya et al. 2012; Li et al. 2009; Shi et al. 2014; Stope et al. 2002). A few studies have shown that several bacteria can degrade DBF via both pathways (Jaiswal et al. 2011; Le et al. 2014; Yamazoe et al. 2004). Bacteria using the angular dioxygenation pathway can easily degrade DBF channeled into the tricarboxylic acid (TCA) cycle (Xu et al. 2006; Additional file 1: Figure S1), while bacteria co-metabolizing DBF via lateral

dioxygenation are thought to be unable to degrade DBF completely, because lateral oxidation often leads to dead-end products (Hiraishi 2003). Biotechnologies such as gene and transcriptome sequencing can be useful in elucidating the genes directly involved in angular dioxygenation pathway (Miller et al. 2010; Nojiri et al. 2002), but the metabolites and enzymes of lateral dioxygenation are more difficult to identify. Studies have shown that enzymes involved in the BP and naphthalene catabolic pathways are likely involved in the co-metabolism of DBF (Mohammadi and Sylvestre 2005; Resnick and Gibson 1996; Seeger et al. 2001; Wesche et al. 2005).

Pseudomonas putida strain B6-2 was isolated and found to transform DBF via a lateral dioxygenation pathway during cultivation with BP (Li et al. 2009; Tang et al. 2011; Yao et al. 2017). First, DBF is mainly attacked at the 1,2-C position by BP-dioxygenase (BphA); then, it is dehydrogenated by BP-dihydrodiol dehydrogenase (BphB) and dioxygenolytically cleaved by dihydroxybiphenyl dioxygenase (BphC) to produce 2-hydroxy-4-(3′-oxo-3′*H*-benzofuran-2′-yliden)but-2-enoic acid (HOBB) (Fig. 1b), which is a major metabolite in the biodegradation pathway (Becher et al. 2000; Hammer et al. 1998; Kaiya et al. 2012; Li et al. 2009; Stope et al. 2002). Some new downstream metabolites of HOBB have been reported (Li et al. 2009; Shi et al. 2013), but the entire pathway and enzymes involved as well as how the resulting metabolites are further degraded remain unclear. Preparation of pure HOBB through biosynthesis and its use as a substrate for screening would provide insight into the lateral dioxygenation pathway. In addition, HOBB, which is a singular heterocycle, may be useful for synthesizing complex benzofuran derivatives with biological activities. If its accumulation could be increased, it would be easier and more convenient to synthesize these bioactive products through subsequent substitution and synthetic reactions.

The use of whole-cell microbial biocatalysts is a promising technique for industrial production (Schmid et al. 2001). Whole-cell biocatalysts provide energy and recycle cofactors in redox reactions (Schmid et al. 2001; Zhao and van der Donk 2003), and have the prospect of becoming powerful tools in organic synthesis (Schrewe et al. 2013). Many studies have attempted to use microorganisms to synthesize valuable compounds (Hsieh et al. 2017; Kadisch et al. 2017; Nikel et al. 2016; Nuland et al. 2017; Wang et al. 2005, 2015; Yu et al. 2014, 2017).

Herein, we describe the development of an environmental-friendly method for biosynthesizing HOBB from DBF using whole cells of *P. putida* strain B6-2. First, different cultivation media were compared to test the biosynthesis. Then, different biosynthesis conditions including pH, optical density at 600 nm (OD_{600}), the initial DBF concentrations, and different extraction conditions were evaluated to achieve the maximum HOBB yield. Finally, batch and fed-batch processes were compared to determine which process makes full use of the bacteria and increases the yield of HOBB.

Methods

Chemicals

Dibenzofuran (98%) was purchased from J & K Chemicals (Beijing, China). HPLC grade formic acid, HPLC grade methanol, and GC grade *N*,*N*-dimethylformamide (DMF) were obtained from Aladdin (Italy). *N*,*O*-bis-(trimethylsilyl)trifluoroacetamide (BSTFA) for GC derivatization was obtained from Sigma-Aldrich (USA). All other reagents and analytical grade chemicals were purchased from Sinopharm Chemical Reagent Co., Ltd (Shanghai, China).

Bacteria and culture conditions

Pseudomonas putida strain B6-2 was isolated from soil and characterized to cometabolize DBF by growing with BP as the sole carbon source as previously described (Li et al. 2009). The strain was deposited at Deutsche Sammlung von Mikroorganismen und Zellkulturen in Gottingen (Germany) under DSM No. 28064. The bacteria were cultivated in lysogeny broth (LB) or mineral salts medium (MSM) (pH 7) containing (per liter distilled water) 5.2-g K_2HPO_4, 3.7-g KH_2PO_4, 0.1-g $MgSO_4$, 1-g Na_2SO_4, 2-g NH_4Cl, and 1-mL trace metal solution (Li et al. 2006). The phosphate buffer (PBS) used to suspend the bacteria was prepared with 1.42-g Na_2HPO_4, 0.27-g KH_2PO_4, 8-g NaCl, and 0.2-g KCl per liter distilled water, and the pH was adjusted with 1-M HCl or 1-M NaOH according to experimental requirements. BP and DBF were separately dissolved in DMF to prepare a mother liquid with a concentration of 100 mM.

Flask cultivation was conducted in 2-L flasks containing 1 L of broth at pH 7, 30 °C, and 200 rpm. Growth curves of strain B6-2 were determined in three different media, including LB medium, LB medium containing 2-mM BP, and MSM containing 10-mM BP, and the ability of B6-2 cells to degrade DBF in each medium was also evaluated.

Preparation for biosynthesis

Strain B6-2 was cultivated in growth medium overnight, harvested at the mid-exponential phase by centrifuging at 6000*g* for 20 min at 4 °C, and then washed three times with PBS. These cells were suspended in PBS to the proper OD_{600} for biosynthesis.

Extraction and analytic methods

Suspended cells (10 mL) and DBF were added into a 50-mL flask to conduct a reaction with shaking (200 rpm) at 30 °C. After the pH was adjusted to 2, ethyl acetate

(5 mL) was added. The metabolites were extracted into the organic phase by shaking and separated by centrifuging and partitioning. Then, the organic phase supernatant was removed, passed through a 0.22-μm filter, and analyzed with high-performance liquid chromatography (HPLC) (Agilent 1200 series, Agilent Technologies Inc., USA).

Different DBF concentrations (0.3, 0.5, 0.8, and 1.0 mM), pH values (5, 7, 8, and 9) and OD_{600} values (2, 5, and 10) were studied to identify the best reaction conditions of all trials. The extraction efficiencies of different extractants including cyclohexane, dichloromethane, trichloromethane, butanol, and ethyl acetate were also tested. In addition, two different extraction methods for preparing HOBB were also compared. For the acid–alkali-acid method, the pH was adjusted to 2, and the solution was first extracted with equivoluminal organic solvent, then the organic phase was extracted with 1/2 volume water (pH 10), and finally, after pH was adjusted to 2, the aqueous phase was extracted again with equivoluminal organic solvent. For the neutral-acid extraction method, the reaction liquid was directly extracted with an organic extractant, then the pH was adjusted to 2, and the reaction liquid was extracted again. The final organic phase was used for the detection and preparation of HOBB.

The HPLC system was equipped with a ZORBAX-C18 column (150 mm × 4.6 mm, 5 μm, Agilent Technologies Inc., USA) and a diode-array detector (DAD). DBF was detected at a wavelength of 280 nm, and HOBB was detected at 405 nm. To obtain quantitative data, a volume of 5 μL was injected into the system and eluted with a mixture of methanol and water (1‰ HCOOH) over 56 min. The initial percentages of methanol and water were 30 and 70% (v/v), respectively, with a flow rate 0.5 mL/min. The methanol gradient then increased to 50% over 5 min, increased to 90% over the next 30 min, was maintained at 90% for 10 min, and, finally, decreased to 30% over 1 min. The column was then balanced for another 9 min.

LC–MS/TOF accurate mass analysis (Agilent 6230, USA) was performed using a similar elution procedure with a flow rate of 0.4 mL/min. The MS was equipped with a standard ESI in the negative ion mode, and N_2 was used as a sheath gas (40 psi).

Purified HOBB was dissolved in DMSO and then derivatized with BSTFA at 70 °C for 45 min (Jaiswal et al. 2011). After derivatization, GC–MS was conducted using conditions similar to those previously described (Li et al. 2009). NMR spectra were obtained for solutions in DMSO-d_6 on an Avance 600 spectrometer (Bruker) operated at 600 MHz for ^{1}H and at 150 MHz for ^{13}C. H–H COSY, HMBC, and HSQC spectra of silylated HOBB were recorded.

Biosynthesis and preparation of HOBB

Biosynthesis was conducted with 200 mL of the bacterial culture in a 1-L flask under the best conditions determined from all trials. Two strategies were used for biosynthesis. After the DBF biodegradation rate decreased, cells were harvested by centrifugation and recycled into a fresh batch reaction. This was repeated a second time for a total of three recycled batch processes with the same biocatalysts. For the fed-batch process, DBF was supplemented with the same concentrations as the batch group at the same time.

After the reaction was complete, cells were harvested by centrifugation and the supernatant was extracted with the best extraction method of all trials. After the organic phase was collected and condensed, crude HOBB was obtained. Further purification was conducted by washing the sediment several times with a small amount of ethyl acetate, and the sample was dried with nitrogen blowing and then freeze-dried to a constant weight. Purified HOBB was dissolved in DMF and diluted with ethyl acetate to generate a standard curve for HPLC, LC–MS, and GC–MS analysis.

Statistical analysis

All experiments were conducted for three replicates. Data were analyzed using Microsoft Excel and Origin 8.0 for Windows. Results are reported as the mean ± SD.

Results

Preparation for biosynthesis

Strain B6-2 was cultured in three different media, including LB medium, LB medium containing 2 mM BP, and MSM containing 10 mM BP. Cells were harvested, washed, and suspended in PBS (pH 7.5) to an OD_{600} of 5. Growth, degradation of DBF, and accumulation of HOBB in the three media were compared. The growth rate and biomass of strain B6-2 cultivated in LB medium and LB medium containing BP were higher than those of the strain cultivated in MSM medium containing BP (Fig. 2a). The fastest rates of DBF degradation and HOBB accumulation were observed in whole cells prepared from LB medium containing BP, followed by cells prepared from MSM containing BP and LB medium (Fig. 2b). Therefore, strain B6-2 was cultured in LB medium containing BP in subsequent experiments.

Reaction conditions for biosynthesis

The effect of the initial substrate concentration on HOBB synthesis was evaluated next (Fig. 3a). Strain B6-2 cultivated in LB medium containing 2 mM BP was harvested and suspended in PBS (pH 7.5) to an OD_{600} of 5. When 0.3 mM DBF was added, it was completely degraded in 4 h, and the highest amount of HOBB obtained was approximately 0.14 mM. When the starting concentration was 0.5 mM, DBF was almost completely degraded and a large amount of HOBB (~ 0.26 mM) was produced

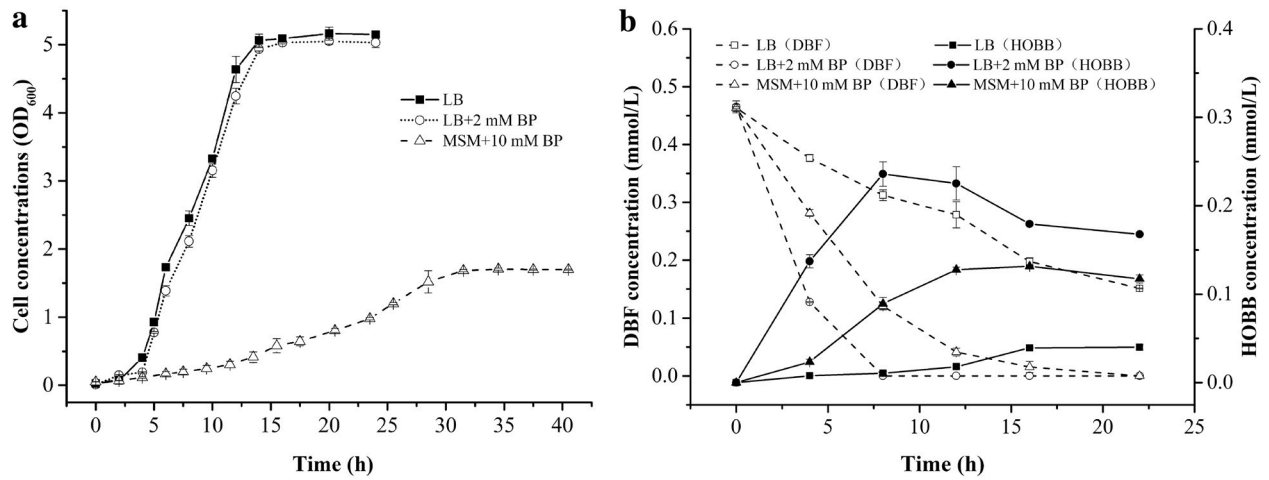

Fig. 2 Preparation of biocatalyst using different media. **a** Growth curves of strain B6-2 in three different media: LB medium (closed square), LB medium with 2-mM BP (open circle), and MSM with 10-mM BP (open triangle). **b** DBF degradation (dotted line) in LB medium (open square), LB medium with 2-mM BP (open circle) and MSM with 10-mM BP (open triangle), and HOBB accumulation (solid line) in LB medium (closed square), and LB medium with 2-mM BP (closed circle) and MSM with 10-mM BP (closed triangle) after cultivation of strain B6-2

by 8 h. With starting concentrations of 0.8 mM and 1.0 mM, DBF was not completely degraded; only approximately 0.5 mM DBF was degraded after 22 h. Though the amount of HOBB was the highest at 12 and 16 h for starting concentrations of 0.8-mM and 1.0-mM DBF, respectively, the highest amount of HOBB obtained from the both groups were lower than the highest amount obtained with a starting concentration of 0.5 mM. Based on the results shown in Fig. 3a, the initial rates of DBF degradation during the first 4 h were 0.072 mM h^{-1} ($C_{initial}$ = 0.3-mM DBF), 0.074 mM h^{-1} ($C_{initial}$ = 0.5-mM DBF), 0.067 mM h^{-1} ($C_{initial}$ = 0.8-mM DBF) and 0.044 mM h^{-1} ($C_{initial}$ = 1.0-mM DBF). Almost the same rates of DBF degradation were observed when the starting concentrations were 0.3 mM and 0.5 mM. However, the rate of DBF degradation decreased as the starting DBF concentration increased from 0.5 to 0.8 mM and from 0.8 to 1.0 mM. Therefore, it can be concluded that high concentrations of DBF (i.e., starting concentrations of 0.8 and 1.0 mM) slow down the rate of DBF degradation and HOBB accumulation (Fig. 3a). Furthermore, with starting concentrations of 0.8- and 1.0-mM DBF under the conditions of OD_{600} 5, pH 7.5, strain B6-2 was only able to degrade about 0.5-mM DBF (Fig. 3a). Therefore, 0.5 mM was chosen as the best concentration for HOBB biosynthesis.

To increase the production of HOBB, biosynthesis at different pH values (Fig. 3b) and cell densities (Fig. 3c) was evaluated. After cultivation in LB medium containing 2-mM BP, strain B6-2 was suspended in PBS of different pH values to an OD_{600} of 5, and 0.5-mM DBF was added. Although strain B6-2 can tolerate pH 5, only a small amount of DBF was degraded, and there was barely any HOBB accumulation. In addition, the biosynthesis system did not have the orange color that is characteristic of HOBB in a neutral or alkaline environment. The highest concentration of HOBB was obtained after approximately 8 h at pH 7 (Fig. 3b). When pH increased from 7 to 9, the rate of HOBB accumulation decreased along with the rate of DBF degradation. In terms of cell density, an OD_{600} of 5 clearly led to higher HOBB production than an OD_{600} of 2 in PBS (pH 7.5), and DBF degradation and HOBB accumulation were only minimally different from that observed at an OD_{600} of 10 (Fig. 3c). For groups with an OD_{600} of 5 and 10, 0.5-mM DBF was almost completely degraded after 8 h.

When strain B6-2 was incubated at LB medium containing 2-mM BP and conducted biosynthesis under the best conditions (C_{DBF} = 0.5 mM, OD_{600} of 5, and pH 7) determined from all trials in a volume of 10 mL, DBF was rapidly degraded and HOBB (0.26 ± 0.007 mM) was accumulated by 8 h (Fig. 3d).

Conditions for extraction

Different extractants were applied after biosynthesis and centrifugation. Cyclohexane, dichloromethane, and trichloromethane extracted very little HOBB from the reaction liquid. Better HOBB extraction was obtained with butanol and ethyl acetate (Additional file 1: Table S1). The extraction efficiency of ethyl acetate (0.135 ± 0.003 mM HOBB) was much higher than that of butanol (0.077 ± 0.003 mM HOBB) as determined by HPLC.

The extraction efficiencies of ethyl acetate using two different extraction methods (acid–alkali-acid method

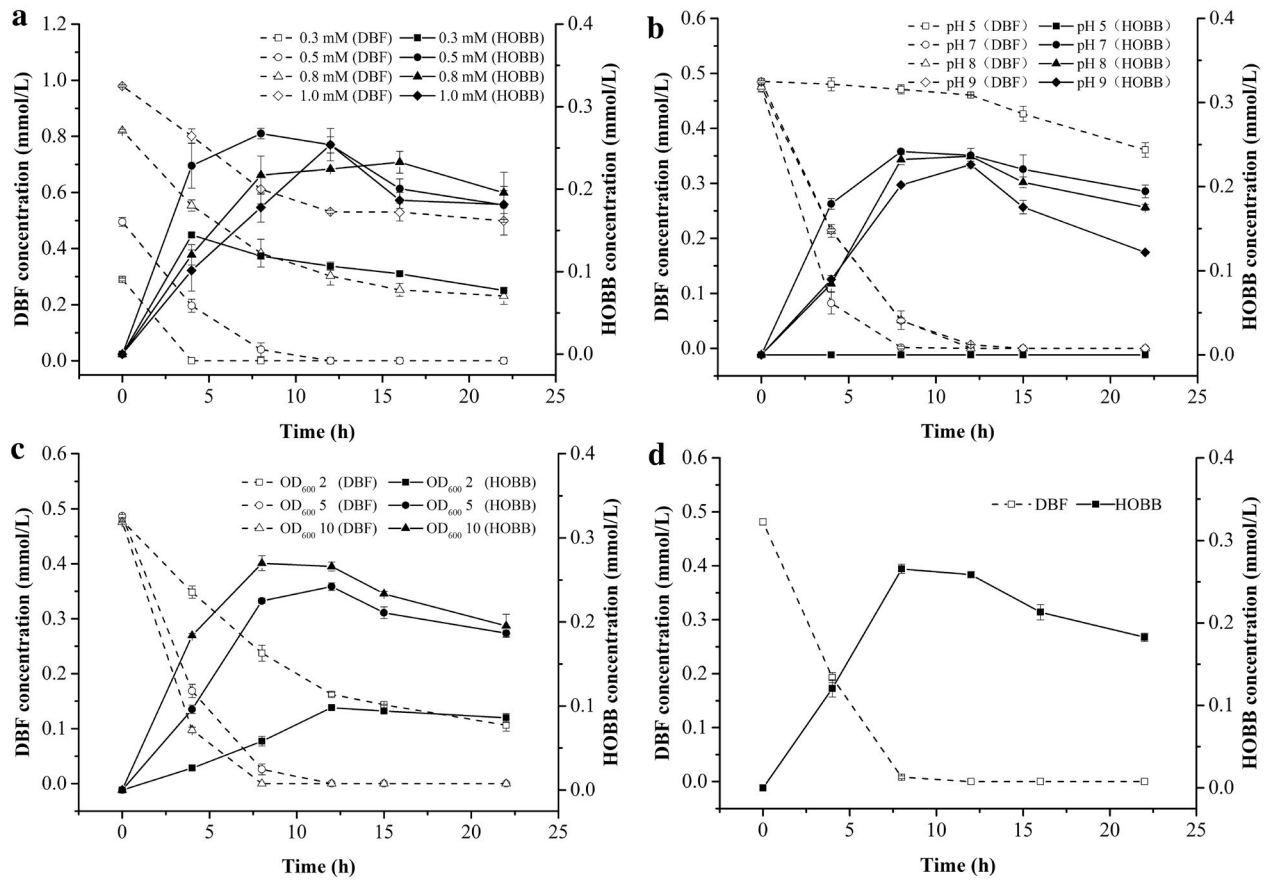

Fig. 3 Trials of biosynthesis conditions. DBF degradation (dotted line) and HOBB accumulation (solid line) were evaluated under different conditions. **a** Initial DBF concentration. DBF degradation: 0.3-mM DBF (open square), 0.5-mM DBF (open circle), 0.8-mM DBF (open triangle), 1.0-mM DBF (open diamond); HOBB accumulation: 0.3-mM DBF (closed square), 0.5-mM DBF (closed circle), 0.8-mM DBF (closed triangle), and 1.0-mM DBF (closed diamond). **b** Different pH values. DBF degradation: pH 5 (open square), pH 7 (open circle), pH 8 (open triangle), pH 9 (open diamond); HOBB accumulation: pH 5 (closed square), pH 7 (closed circle), pH 8 (closed triangle), pH 9 (closed diamond). **c** Cells density. DBF degradation: OD_{600} 2 (open square), OD_{600} 5 (open circle), OD_{600} 10 (open triangle); HOBB accumulation: OD_{600} 2 (closed square), OD_{600} 5 (closed circle), and OD_{600} 10 (closed triangle). **d** DBF degradation (open square) and HOBB accumulation (closed square) under the best conditions among all trials: OD_{600} 5, pH 7, and $C_{DBF} = 0.5$ mM in a 10-mL system

and neutral-acid method) were determined by HPLC. Both methods removed residual DBF and upstream products of HOBB biosynthesis (Fig. 1b). Approximately 0.072 ± 0.0001-mM HOBB was obtained with the acid–alkali-acid method, and compared to direct extraction (0.135 ± 0.003 mM HOBB), the extraction efficiency was 53.1%. The neutral-acid method yielded 0.096 ± 0.002 mM HOBB with an extraction efficiency of 70.8%. Therefore, extraction with ethyl acetate using the neutral-acid method is a better extraction method.

Detection and verification of HOBB and DBF

DBF was easily identified by HPLC at 280 nm using standards. HOBB was first separated and identified using LC–MS (Fig. 4a). A molecular ion peak (M^-) at *m/z* 231.0295 (RT 18.337 min, $\lambda = 405$ nm) corresponded to $C_{12}H_8O_5$ (theoretical: 231.0299), and possessed exactly the same UV–vis spectra as HOBB in the acid mobile phase (Stope et al. 2002). HOBB cannot be detected on GC–MS unless it is derived, so HOBB was silylated before analysis. One major peak at RT 18.1 min (Fig. 4b) had a molecular weight of 376 and main ion peaks at *m/z* 376, 259, 147 and 73, which indicated that HOBB was successfully silylated on hydroxyl and carboxylic acid groups. NMR spectra of ^1H and ^{13}C (Table 1) suggest the structure shown in Fig. 4c, and are consistent with those previously reported by Stope et al. (2002). Taken together, these results confirmed that the purified metabolite was HOBB.

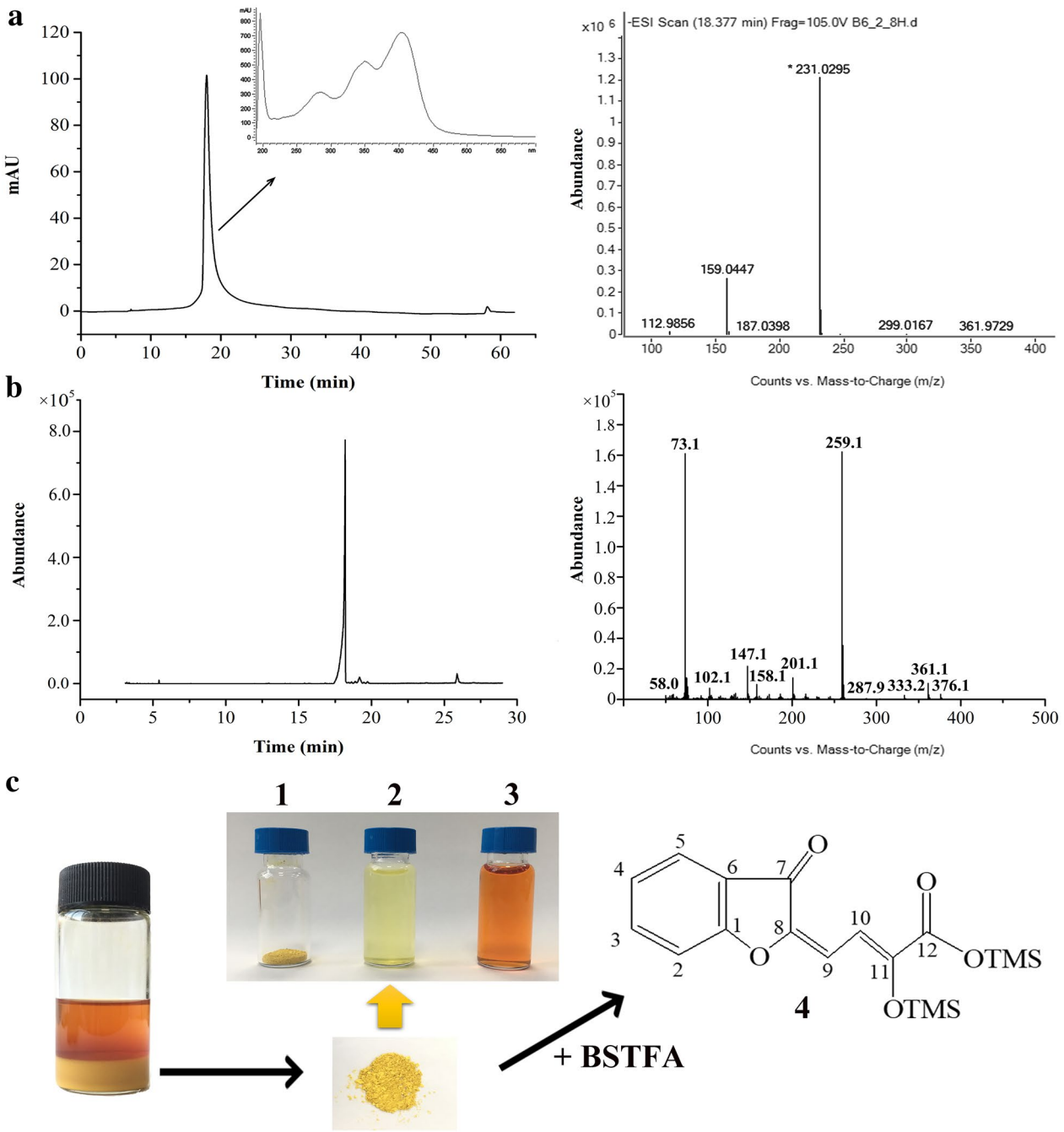

Fig. 4 Preparation and identification of HOBB by mass spectra and NMR analysis. **a** HPLC detection revealed a peak at RT 18.377 min ($\lambda = 405$ nm) with UV–Vis spectra in the acid mobile phase, and mass spectra verification revealed a molecular ion peak (M^-) at *m/z* 231.0299 ($C_{12}H_8O_5$) consistent with HOBB. **b** GC–MS detection of silylated HOBB (derived with BSTFA) with one major peak at RT 18.1 min, showing main ion peaks at *m/z* 376, 259, 147 and 73. **c** When preparing HOBB, the sediment was purified by washing with a small amount of ethyl acetate. Purified HOBB was a yellow powder (**1**). This powder turned yellow–green in color when dissolved in ethyl acetate (**2**) and dark-orange in color when dissolved in DMF (**3**). The structure of silylated HOBB was determined by NMR analysis (derived with BSTFA) (**4**)

Table 1 ^{1}H NMR (600 MHz) and ^{13}C NMR (150 MHz) results for silylated HOBB in DMSO-d_6

δ (ppm)	Proton assignment	J (Hz)	δ (ppm)	Carbon assignment
6.468	H-9, d	^{3}J = 12.2	106.32	C-10
6.698	H-10, d	^{3}J = 12.2	112.26	C-9
7.065	H-4, t	^{3}J = 7.4	113.91	C-2
7.231	H-2, d	^{3}J = 8.2	122.32	C-6
7.518	H-3, t	^{3}J = 7.4	124.81	C-4
7.543	H-5, d	^{3}J = 7.3	125.07	C-3
			138.54	C-5
			147.69	C-8
			148.76	C-11
			163.92	C-12
			165.82	C-1
			183.42	C-7

Biosynthesis and preparation of HOBB

After cultivation in LB medium containing 2-mM BP, strain B6-2 was used for biosynthesis under the best conditions determined from the trials (OD_{600} of 5 and pH 7). To improve yield, batch and fed-batch processes were performed in 1-L bottles containing 200-mL reaction liquid.

For the batch process, the biocatalyst was recycled and used in three sequential batch reactions (Fig. 5a). The initial concentration of DBF was 0.5 mM. When about 0.45-mM DBF was degraded (~8.5 h) in the first batch, cells were harvested by centrifugation and reused to convert 0.4-mM DBF in another batch reaction. When approximately 0.25-mM DBF was degraded and almost no HOBB was further accumulated (~18 h) in the second batch, cells were reused again to convert a new batch reaction of 0.3-mM DBF. In addition, almost no DBF was degraded in the third batch (Fig. 5a). The yields of HOBB obtained from conversion of DBF in the first two batch steps were 0.21 ± 0.01 mM (48.3%) and 0.079 ± 0.003 mM (34.4%), respectively.

For the fed-batch process, DBF was added into the same bio-reaction system for three times and HOBB remained in the bioreactor until the end of the run. To make a contrast with batch process, 0.5-mM DBF was used as the initial concentration, 0.4-mM DBF was added into the reaction system at 8.5 h, and 0.3-mM DBF was supplemented at 26.5 h (Fig. 5b).

The rate of DBF degradation and HOBB accumulation in the batch and fed-batch processes slowed down after adding 0.4-mM DBF. Compared with a single step, in which about 0.5-mM DBF was degraded (Fig. 3a), the use of batch biosynthesis, in which bacteria were utilized twice, increased the amount of DBF degraded to about 0.7 mM. The highest concentration of HOBB obtained in the fed-batch group was 0.24 ± 0.006 mM at 21 h (Fig. 5b), which was lower than the yield of the batch biosynthesis (0.29 ± 0.003 mM).

The supernatant of the first two batch groups was collected to prepare HOBB, and the crude product containing a mixture of red–brown and yellow compounds was obtained after extraction. After washing with a small amount of ethyl acetate, the supernatant was brown, while the sediment was yellow (Fig. 4c). Pure HOBB, which is a yellow powder, was then obtained (Fig. 4c-1). About 13.58 ± 0.31 mg of HOBB was obtained from

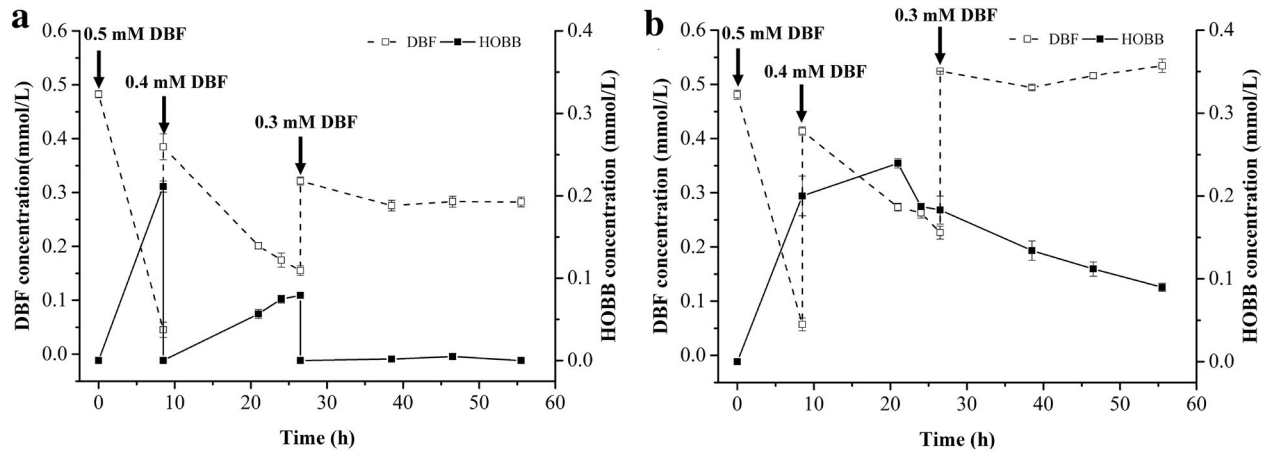

Fig. 5 Biosyntheses of HOBB in batch and fed-batch processes. DBF degradation (open square) and HOBB accumulation (closed square) were evaluated in the two groups. **a** For the batch group, the biocatalysts were recycled twice, so that there were three sequential batch processes. The initial DBF concentration was 0.5 mM. After DBF was almost completely degraded at 8.5 h, bacteria were recycled by centrifugation and reused for another batch biosynthesis with 0.4-mM DBF. When almost no DBF was degraded, bacteria were reused again for another batch biosynthesis with 0.3-mM DBF. **b** For the fed-batch group, the same concentrations of DBF were added directly into the reaction systems at the same time as batch group

22.49 ± 0.74 mg DBF with a high overall production yield of 60.4% (w/w). This powder became yellow–green in color when dissolved in ethyl acetate (Fig. 4c-2), and presented dark-orange in color when dissolved in DMF (Fig. 4c-3). The powder was more easily dissolved in DMF than in ethyl acetate. The purified HOBB was used as the standard to quantify yield.

Discussion

Compounds with a benzofuran nucleus have a wide range of therapeutic effects (Khanam and Shamsuzzaman 2015), acting as potent anti-tumor, antimicrobial, and antiviral agents. The synthesis of these compounds from benzofuran derivatives has been widely studied (El-Zahar et al. 2011; Galal et al. 2009; Ma et al. 2016). To obtain these products, benzofuran rings must be chemically synthesized; however, some of these syntheses require expensive catalysts, such as the noble metals Pd (Oppenheimer et al. 2007; Trost and Mcclory 2007) and Rh (Cacchi et al. 2002), and require strict operational conditions. This study reveals an easier and more convenient strategy to synthesize the benzofuran derivative HOBB using whole cells of a *P. putida* strain.

DBF can be catabolized by *P. putida* B6-2 via two pathways (Fig. 1b), with the major pathway leading to the accumulation of HOBB (Li et al. 2009). According to accumulation curves (Fig. 3), the amount of HOBB increased rapidly reaching a maximum level and then slightly decreased in a short period of time. Thus, strain B6-2 is a good choice for HOBB biosynthesis. It can also be inferred that the level of HOBB accumulation is determined by the balance between production and degradation. The color of the reaction system rapidly turned from white to orange, stayed orange for a period of time, and finally deepened in color, suggesting that HOBB might be transformed into other metabolites. Consistent with this color change, HPLC analysis also revealed a decrease in HOBB concentration.

Cultivation media affect how much DBF is degraded and how much HOBB accumulates (Fig. 2b). This is likely because some enzymes involved in DBF degradation such as BphA, BphB, and BphC are not induced in LB medium, thus decreasing the rate of DBF degradation. Adding BP to the LB medium can overcome this problem, because it activates degradation-related genes when bacteria grow rapidly.

Higher concentrations of DBF (0.8 and 1.0 mM) can slow the HOBB biosynthesis reaction (Fig. 3a). In addition, during the batch synthesis, the degradation activity of strain B6-2 declined dramatically after adding 0.4-mM DBF (Fig. 5a). This might be due to the fact that DBF and its metabolites are toxic and can inhibit degradation. Therefore, using a proper DBF concentration matters a lot in achieving efficient degradation. In addition, the pH of the solution impacts the efficiency of DBF degradation. A pH of 5 was tested, because our lab previously showed that strain B6-2 can tolerate this condition. Based on the low yield of HOBB at this pH and compared with the high yield at other pH values (7, 8 and 9) (Fig. 3b), it can be inferred that a neutral or slightly alkaline medium facilitates DBF degradation and HOBB accumulation. However, as pH increased from 7 to 9, the highest production of HOBB decreased (Fig. 3b). This may be because an alkaline environment makes HOBB unstable due to its unsaturated structure. Therefore, pH 7 is preferred over other pH values. After the best culturing conditions of trials for HOBB production were established, the efficiencies of different extractants were tested. Similar substances can dissolve each other; therefore, different extractants have different extraction efficiencies. Ethyl acetate has a polarity similar to that of HOBB, which increases its extraction efficiency compared with that of butanol.

After purification of HOBB, HPLC analysis was done to assess purity. Except for the solvent peak, only single peaks were observed at 210, 235, 254, 280, 300, 350, and 405 nm (reference = 600 nm) (Additional file 1: Figure S2). The peak areas corresponding to HOBB in HPLC and GC–MS chromatograms were greater than 95%, and thus, the product was recognized to be pure and could be quantified. As HOBB shows a keto-enol tautomerism (Stope et al. 2002), it is difficult to directly determine its structure by GC–MS and NMR. Therefore, we elucidated the molecular structure through NMR analysis of a derivatized form, silylated HOBB (Fig. 4c-4).

Equimolar conversion of DBF to HOBB could not be achieved (Figs. 2 and 3). There are a few possible explanations for this. First, although the pathway leading to HOBB accumulation is the major pathway, DBF can be also consumed by a minor pathway to produce another product called 4-(2-hydroxy-3-benzofuranyl)-2-oxo-3-butenoic acid (Fig. 1b). Second, strain B6-2 can degrade HOBB during the whole process of biosynthesis. Third, the properties of HOBB and DBF differ: DBF possesses a weaker polarity, is harder to dissolve in water, and is easier to dissolve in the organic phase than HOBB. Therefore, extraction efficiencies of DBF and HOBB are different. Furthermore, the accuracy of HPLC detection may also differ. Unlike DBF, HOBB, even under acidic mobile phase conditions, has obvious tailed-peaks at low concentrations (such as below 0.1 mM), which will affect the integrated results.

Very different results were observed when biosyntheses were performed using the batch and fed-batch processes. The same amount of bacteria transformed more DBF and synthesized more HOBB in the batch group than in the

fed-batch group (Fig. 5). After adding 0.3-mM DBF at 26.5 h, the bacteria in the fed-batch process almost completely lost the ability to degrade DBF, and the concentration of HOBB decreased. It can be inferred that if HOBB is present in the reaction system for a long time, it will become unstable and will be transformed into other by-products. HOBB may also cause the product inhibition. Therefore, centrifuging the supernatant and resuspending in new media prior to conducting a new round of biosynthesis will help to increase the accumulation of HOBB and make the full use of the bacteria.

Conclusions

In summary, a pharmacological value-added compound HOBB was biosynthesized from DBF using whole cells of *P. putida* B6-2 via the lateral dioxygenation pathway, and a high overall production yield (60.4%, w/w) was obtained. The biosynthesis of HOBB may provide a new green route for synthesizing benzofuran derivatives with pharmacological activities.

Additional file

Additional file 1. Supplemrntary figures and table.

Authors' contributions

LX and TH conceived and designed the experiments. LX, WW, HH, LX, and ZL performed the experiments and analyzed the data. LX and TH wrote the paper. LX, XP, and TH revised the manuscript. All authors read and approved the final manuscript.

Acknowledgements

Not applicable.

Competing interests

The authors declare that they have no competing interests.

Availability of data and materials

All data generated or analyzed during this study are included in the main manuscript file.

Consent for publication

The authors approved the consent for publishing the manuscript.

Ethics approval and consent to participate

Not applicable.

Funding

This work was supported by grants from the Chinese National Science Foundation for Excellent Young Scholars (31422004), and by the grants from the Science and Technology Commission of Shanghai Municipality (17JC1403300), and by the 'Shuguang Program' (17SG09) supported by Shanghai Education Development Foundation and Shanghai Municipal Education Commission.

Publisher's Note

Received: 12 March 2018 Accepted: 12 May 2018
Published online: 21 May 2018

References

Aswathanarayanappa C, Bheemappa E, Bodke YD, Bhovi VK, Ningegowda R, Shivakumar MC, Peethambar SK, Telkar S (2013) 5-Phenyl-1-benzofuran-2-yl derivatives: synthesis, antimicrobial, and antioxidant activity. Med Chem Res 22(1):78–87. https://doi.org/10.1007/s00044-012-0017-y

Becher D, Specht M, Hammer E, Francke W, Schauer F (2000) Cometabolic degradation of dibenzofuran by biphenyl-cultivated *Ralstonia* sp. strain SBUG 290. Appl Environ Microbiol 66(10):4528–4531. https://doi.org/10.1128/aem.66.10.4528-4531.2000

Cacchi S, Fabrizi G, Goggiomani A (2002) Palladium catalysis in the construction of the benzo[*b*]furan and furan rings from alkynes and organic halides or triflates. Heterocycles 56(1):613–632. https://doi.org/10.1002/chin.200213262

El-Zahar MI, El-Karim SSA, Haiba ME, Khedr MA (2011) Synthesis, antitumor activity and molecular docking study of novel benzofuran-2-yl pyrazole pyrimidine derivatives. Acta Pol Pharm 68(3):357–373

Galal SA, El-All ASA, Abdallah MM, El-Diwani HI (2009) Synthesis of potent antitumor and antiviral benzofuran derivatives. Bioorg Med Chem Lett 19(9):2420–2428. https://doi.org/10.1016/j.bmcl.2009.03.069

Hammer E, Krowas D, Schäfer A, Specht M, Francke W, Schauer F (1998) Isolation and characterization of a dibenzofuran-degrading yeast: identification of oxidation and ring cleavage products. Appl Environ Microbiol 64(6):2215–2219

Hayakawa I, Shioya R, Agatsuma T, Furukawa H, Sugano Y (2004a) Thienopyridine and benzofuran derivatives as potent anti-tumor agents possessing different structure-activity relationships. Bioorg Med Chem Lett 14(13):3411–3414. https://doi.org/10.1016/j.bmcl.2004.04.079

Hayakawa I, Shioya R, Agatsuma T, Furukawa H, Naruto S, Sugano Y (2004b) 4-Hydroxy-3-methyl-6-phenylbenzofuran-2-carboxylic acid ethyl ester derivatives as potent anti-tumor agents. Bioorg Med Chem Lett 14(2):455–458. https://doi.org/10.1016/j.bmcl.2003.10.039

Hiraishi A (2003) Biodiversity of dioxin-degrading microorganisms and potential utilization in bioremediation. Microbes Environ 18(3):105–125. https://doi.org/10.1264/jsme2.18.105

Hong HB, Nam IH, Murugesan K, Kim YM, Chang YS (2004) Biodegradation of dibenzo-*p*-dioxin, dibenzofuran, and chlorodibenzo-*p*-dioxins by *Pseudomonas veronii* PH-03. Biodegradation 15(5):303–313. https://doi.org/10.1023/B:BIOD.0000042185.04905.0d

Hsieh SC, Wang JH, Lai YC, Su CY, Lee KT (2017) Production of 1-dodecanol, 1-tetradecanol, and 1,12-dodecanediol by whole-cell biotransformation in *Escherichia coli*. Appl Environ Microbiol 84(4):e01806–e01817. https://doi.org/10.1128/AEM.01806-17

Ishige T, Honda K, Shimizu S (2005) Whole organism biocatalysis. Curr Opin Chem Biol 9(2):174–180. https://doi.org/10.1016/j.cbpa.2005.02.001

Jaiswal PK, Kohli S, Gopal M, Thakur IS (2011) Isolation and characterization of alkalotolerant *Pseudomonas* sp. strain ISTDF1 for degradation of dibenzofuran. J Ind Microbiol Biotechnol 38(4):503–511. https://doi.org/10.1007/s10295-010-0793-7

Judd DB, Cardwell KS, Panchal TA, Jack TI, Pass M, Hubbard T, Dean AW, Butt AU, Hobson JE, Heron NM, Watson SP, Currie GS, Middlemiss D, Allen DG, Aston NM, Paton JMS, Drew GM, Hilditch A, Gallacher D, Bayliss MK, Donnelly MC (1994) Benzofuran based non-peptide antagonists of angiotensin II related to GR117289: part IV; imidazopyridinylbenzofurans. Bioorg Med Chem Lett 4(5):725–728. https://doi.org/10.1016/S0960-894X(01)80188-8

Kadisch M, Julsing MK, Schrewe M, Jehmlich N, Scheer B, Von Bergen M, Schmid A, Buhler B (2017) Maximization of cell viability rather than biocatalyst activity improves whole-cell ω-oxyfunctionalization performance. Biotechnol Bioeng 114(4):874–884. https://doi.org/10.1002/bit.26213

Kaiya S, Utsunomiya S, Suzuki S, Yoshida N, Futamata H, Yamada T, Hiraishi A (2012) Isolation and functional gene analyses of aromatic-hydrocarbon-degrading bacteria from a polychlorinated-dioxin-dechlorinating process. Microbes Environ 27(2):127–135. https://doi.org/10.1264/jsme2.ME11283

Khanam H, Shamsuzzaman (2015) Bioactive benzofuran derivatives: a review. Eur J Med Chem 97:483–504. https://doi.org/10.1016/j.ejmech.2014.11.039

Le TT, Murugesan K, Nam IH, Jeon JR, Chang YS (2014) Degradation of dibenzofuran via multiple dioxygenation by a newly isolated *Agrobacterium*

sp. PH-08. J Appl Microbiol 116(3):542–553. https://doi.org/10.1111/jam.12403
Li L, Li QG, Li FL, Shi Q, Yu B, Liu FR, Xu P (2006) Degradation of carbazole and its derivatives by a *Pseudomonas* sp. Appl Microbiol Biotechnol 73(4):941–948. https://doi.org/10.1007/s00253-006-0530-3
Li QG, Wang XY, Yin GB, Gai ZH, Tang HZ, Ma CQ, Deng ZX, Xu P (2009) New metabolites in dibenzofuran cometabolic degradation by a biphenyl-cultivated *Pseudomonas putida* strain B6-2. Environ Sci Technol 43(22):8635–8642. https://doi.org/10.1021/es901991d
Ma YL, Zheng X, Gao H, Wan CP, Rao GX, Mao ZW (2016) Design, synthesis, and biological evaluation of novel benzofuran derivatives bearing *N*-aryl piperazine moiety. Molecules 21(12):1684. https://doi.org/10.3390/molecules21121684
Matsumura F, Benezet HJ (1973) Studies on the bioaccumulation and microbial degradation of 2,3,7,8-tetrachlorodibenzo-*p*-dioxin. Environ Health Perspect 5:253–258
Miller TR, Delcher AL, Salzberg SL, Saunders E, Detter JC, Halden RU (2010) Genome sequence of the dioxin-mineralizing bacterium *Sphingomonas wittichii* RW1. J Bacteriol 192(22):6101–6102. https://doi.org/10.1128/JB.01030-10
Mohammadi M, Sylvestre M (2005) Resolving the profile of metabolites generated during oxidation of dibenzofuran and chlorodibenzofurans by the biphenyl catabolic pathway enzymes. Chem Biol 12(7):835–846. https://doi.org/10.1016/j.chembiol.2005.05.017
Nevagi RJ, Dighe SN, Dighe SN (2015) Biological and medicinal significance of benzofuran. Eur J Med Chem 97:561–581. https://doi.org/10.1016/j.ejmech.2014.10.085
Nikel PI, Chavarría M, Danchin A, De Lorenzo V (2016) From dirt to industrial applications: *Pseudomonas putida*, as a synthetic biology chassis, for hosting harsh biochemical reactions. Curr Opin Chem Biol 34:20–29. https://doi.org/10.1016/j.cbpa.2016.05.011
Nojiri H, Kamakura M, Urata M, Tanaka T, Chung JS, Takemura T, Yoshida T, Habe H, Omori T (2002) Dioxin catabolic genes are dispersed on the *Terrabacter* sp. DBF63 genome. Biochem Biophys Res Commun 296(2):233–240. https://doi.org/10.1016/S0006-291X(02)00873-2
Nuland YMV, Vogel FAD, Eggink G, Weusthuis RA (2017) Expansion of the ω-oxidation system AlkBGTL of *Pseudomonas putida* GPo1 with AlkJ and AlkH results in exclusive mono-esterified dicarboxylic acid production in *E. coli*. Microb Biotechnol 10(3):594–603. https://doi.org/10.1111/1751-7915.12607
Oppenheimer J, Johnson WL, Tracey MR, Hsung RP, Yao PY, Liu R, Zhao K (2007) A rhodium(I)-catalyzed demethylation-cyclization of o-anisole-substituted ynamides in the synthesis of chiral 2-amido benzofurans. Org Lett 9(12):2361–2364. https://doi.org/10.1021/ol0707362
Resnick SM, Gibson DT (1996) Regio- and stereospecific oxidation of fluorene, dibenzofuran, and dibenzothiophene by naphthalene dioxygenase from *Pseudomonas* sp. strain NCIB 9816-4. Appl Environ Microbiol 62(11):4073–4080
Ritchie G (2000) Dioxin sources and industrial emissions control—a review. Int J Environ Stud 58(1):99–116. https://doi.org/10.1080/00207230008711319
Salih KSM, Ayoub MT, Saadeh HA, Al-Masoudi NA, Mubarak MS (2007) Synthesis, characterization, and biological activities of new benzofuran derivatives. Heterocycles 71(7):1577–1587. https://doi.org/10.1002/chin.200743111
Schmid A, Dordick JS, Hauer B, Kiener A, Wubbolts M, Witholt B (2001) Industrial biocatalysis today and tomorrow. Nature 409(6817):258–268. https://doi.org/10.1038/35051736
Schrewe M, Julsing MK, Buehler B, Schmid A (2013) Whole-cell biocatalysis for selective and productive C-O functional group introduction and modification. Chem Soc Rev 42(15):6346–6377. https://doi.org/10.1039/c3cs60011d
Seeger M, Cámara B, Hofer B (2001) Dehalogenation, denitration, dehydroxylation, and angular attack on substituted biphenyls and related compounds by a biphenyl dioxygenase. J Bacteriol 183(12):3548–3555. https://doi.org/10.1128/JB.183.12.3548-3555.2001
Shi SN, Zhang XW, Ma F, Sun TH, Li A, Zhou JT, Qu YY (2013) Cometabolic degradation of dibenzofuran by *Comamonas* sp. MQ. Process Biochem 48(10):1553–1558. https://doi.org/10.1016/j.procbio.2013.07.003
Shi SN, Qu YY, Fang M, Zhou JT (2014) Bioremediation of coking wastewater containing carbazole, dibenzofuran, dibenzothiophene and naphthalene by a naphthalene-cultivated *Arthrobacter* sp. W1. Bioresour Technol 164:28–33. https://doi.org/10.1016/j.biortech.2014.04.010
Stope MB, Becher D, Hammer E, Schauer F (2002) Cometabolic ring fission of dibenzofuran by gram-negative and gram-positive biphenyl-utilizing bacteria. Appl Microbiol Biotechnol 59(1):62–67. https://doi.org/10.1007/s00253-002-0979-7
Tang HZ, Yu H, Li QG, Wang XY, Gai ZH, Yin GB, Su F, Tao F, Ma C, Xu P (2011) Genome sequence of *Pseudomonas putida* strain B6-2, a superdegrader of polycyclic aromatic hydrocarbons and dioxin-like compounds. J Bacteriol 193(23):6789–6790. https://doi.org/10.1128/JB.06201-11
Trost BM, Mcclory A (2007) Rhodium-catalyzed cycloisomerization: formation of indoles, benzofurans, and enol lactones. Angew Chem Int Ed Engl 46(12):2074–2077. https://doi.org/10.1002/anie.200604183
Wang SN, Xu P, Tang HZ, Meng J, Liu XL, Qing C (2005) "Green" route to 6-hydroxy-3-succinoyl-pyridine from (*S*)-nicotine of tobacco waste by whole cells of a *Pseudomonas* sp. Environ Sci Technol 39(17):6877–6880
Wang WW, Xu P, Tang HZ (2015) Sustainable production of valuable compound 3-succinoyl-pyridine by genetically engineering *Pseudomonas putida* using the tobacco waste. Sci Rep 5:16411. https://doi.org/10.1038/srep16411
Ward CT, Matsumura F (1978) Fate of 2,3,7,8-tetrachlorodibenzo-*p*-dioxin (TCDD) in a model aquatic environment. Arch Environ Contam Toxicol 7(3):349–357. https://doi.org/10.1007/BF02332062
Wesche J, Hammer E, Becher D, Burchhardt G, Schauer F (2005) The *bphC* gene-encoded 2,3-dihydroxybiphenyl-1,2-dioxygenase is involved in complete degradation of dibenzofuran by the biphenyl-degrading bacterium *Ralstonia* sp. SBUG 290. J Appl Microbiol 98(3):635–645. https://doi.org/10.1111/j.1365-2672.2004.02489.x
Wilkes H, Wittich RM, Timmis KN, Fortnagel P, Francke W (1996) Degradation of chlorinated dibenzofurans and dibenzo-*p*-dioxins by *Sphingomonas* sp. strain RW1. Appl Environ Microbiol 62(2):367–371
Wittich RM (1998) Degradation of dioxin-like compounds by microorganisms. Appl Microbiol Biotechnol 49(5):489–499. https://doi.org/10.1007/s002530051203
Wittich RM, Wilkes H, Sinnwell V, Francke W, Fortnagel P (1992) Metabolism of dibenzo-*p*-dioxin by *Sphingomonas* sp. strain RW1. Appl Environ Microbiol 58(3):1005–1010
Xu P, Yu B, Li FL, Cai XF, Ma CQ (2006) Microbial degradation of sulfur, nitrogen and oxygen heterocycles. Trends Microbiol 14(9):398–405. https://doi.org/10.1016/j.tim.2006.07.002
Yamazoe A, Yagi O, Oyaizu H (2004) Degradation of polycyclic aromatic hydrocarbons by a newly isolated dibenzofuran-utilizing *Janibacter* sp. strain YY-1. Appl Microbiol Biotechnol 65(2):211–218. https://doi.org/10.1007/s00253-003-1541-y
Yao XM, Tao F, Zhang KZ, Tang HZ, Xu P (2017) Multiple roles of two efflux pumps in a polycyclic aromatic hydrocarbon-degrading *Pseudomonas putida* strain B6-2 (DSM 28064). Appl Environ Microbiol 83(24):e01882-17. https://doi.org/10.1128/AEM.01882-17
Yeung KS (2012) Furans and benzofurans. In: Gribble GW (ed) Metalation of azoles and related five-membered ring heterocycles. Springer, Berlin Heidelberg, Berlin, pp 47–76. https://doi.org/10.1007/7081_2012_79
Yu H, Tang HZ, Xu P (2014) Green strategy from waste to value-added chemical production: efficient biosynthesis of 6-hydroxy-3-succinoyl-pyridine by an engineered biocatalyst. Sci Rep 4:5397. https://doi.org/10.1038/srep05397
Yu WJ, Wang RS, Li HL, Liang JY, Wang YY, Huang HY, Xie HJ, Wang SN (2017) Green route to synthesis of valuable chemical 6-hydroxynicotine from nicotine in tobacco wastes using genetically engineered *Agrobacterium tumefaciens* S33. Biotechnol Biofuels 10(1):288. https://doi.org/10.1186/s13068-017-0976-9
Zhao H, van der Donk WA (2003) Regeneration of cofactors for use in biocatalysis. Curr Opin Biotechnol 14(6):583–589. https://doi.org/10.1016/j.copbio.2003.09.007